Field Observations of Shallow Freeze and Thaw Processes using High-Frequency Ground-Penetrating Radar

COLBY M. STEELMAN,[1] ANTHONY L. ENDRES,[1] AND JAN VAN DER KRUK[2]

ABSTRACT

Freeze and thaw processes are a fundamental component in cold region hydrology. The depth and distribution of frozen ground in the near-surface can significantly influence the dynamics of surface and subsurface fluid distribution. Seasonal freeze-thaw processes in mid-latitude climates are particularly variable during the course of the winter season and require high resolution monitoring to ensure sufficient temporal and spatial characterization. High-frequency ground-penetrating radar (GPR) is well suited for monitoring the freezing and thawing process in the shallow soil zone due to its non-invasive nature and ability to measure the liquid water component in soil. To illustrate the suitability of high-frequency GPR for monitoring these freezing and thawing processes, 900 MHz common-midpoint (CMP) soundings and reflection profiles were conducted during winter seasonal periods at two separate sites located in Ontario, Canada. The resultant GPR data clearly show the long-term development of a very shallow (<0.5 m) soil frost zone overlying unfrozen wet substratum. Traveltime analysis of these data yielded physical properties of the frozen and unfrozen layers during the course of the winter season as well as the spatial distribution of the base of the soil frost zone. The GPR was also collected during short-term shallow thawing events overlying frozen substratum which resulted in the formation of a dispersive waveguide for both the CMP and reflection profile surveys. Inversion of the dispersive wavefields for the CMP data yielded physical property estimates for the thawed and frozen soils and thawed layer thickness.

Keywords: ground-penetrating radar, seasonal freeze and thaw, frost development, dispersive waveguide

INTRODUCTION

The seasonal freezing and thawing of near-surface sediment is a fundamental component in hydrological processes such as the infiltration of meltwater, surface water runoff and soil water distribution. Knowledge of temporal and spatial distribution of seasonally frozen and thawed zones is the basis for understanding the aforementioned processes because the depth and distribution of these zones significantly influences the dynamics of seasonal soil water content distribution. The seasonal frost zones pertaining to this study are those which form in mid-latitude climates during periods of sub-zero (˚C) atmospheric conditions; these zones are typically constrained to the upper few meters of soil and are exclusively present during the winter seasonal period. Since these seasonal frost zones develop in the near surface, they are susceptible to changes in atmospheric conditions. As a result, seasonal freeze-thaw processes are highly variable

[1] Dep. Earth and Env. Sci., University of Waterloo, Waterloo, ON, N2L 6N6, Canada.
[2] Forschungszentrum Juelich GmbH, ICG4 Agrosphere, D-52425, Juelich, Germany.

during the course of the winter season and require high resolution monitoring to ensure sufficient temporal and spatial characterization.

A comparison of coupled soil water and heat model simulations with field measurements of soil water content, unfrozen water content, soil temperature and drainage water flow by Johnsson and Lundin (1991) showed that the hydraulic complexities associated with seasonal freeze-thaw cycles due to dynamic freezing and thawing of the pore water significantly influence the drainage potential of soils. Field investigations by Nyberg et al. (2001) showed that seasonal soil frost zones can have variable effects on surface runoff dynamics. Further, an extensive field study conducted by Bayard et al. (2005) showed that soil frost formation could significantly reduce the amount of deep percolation and subsequent groundwater recharge by up to 25%. Bayard et al. also demonstrated that surface runoff, subsurface runoff and percolation are primarily influenced by the presence or absence of pore and basal ice. Undoubtedly, field techniques capable of characterizing and monitoring temporal and spatial freeze-thaw processes would provide valuable information for larger-scale hydrological studies examining groundwater and surface water recharge.

Seasonal freeze-thaw processes are typically characterized using invasive point-measurement techniques (e.g., thermistors, frost tubes) which cannot easily be extrapolated to the field-scale. Time-domain reflectometry (TDR) has been shown as an effective technology capable of monitoring the development of seasonal frost zones and subsequent seasonal thaws (e.g., Johnsson and Lundin, 1991; Nyberg et al., 2001; Bayard et al., 2005); the successful application of TDR relies on its ability to infer the liquid water fraction of frozen soil (Patterson and Smith, 1981; Stein and Kane, 1983; Hayhoe and Bailey, 1985). However, TDR requires the installation of numerous horizontally and vertically positioned rods at representative soil depths, limiting its suitability for spatial investigations. On the other hand, relatively non-invasive geophysical methods (e.g., electrical resistivity tomography (ERT), capacitively coupled ERT, electromagnetic induction, ground-penetrating radar) can provide valuable high-resolution information about the spatial distribution and temporal evolution of freeze-thaw processes (Kneisel et al., 2008). Ground-penetrating radar (GPR) is of particular interest in this study due to its unique capabilities of delineating thermal interfaces (i.e., imaging the boundary between frozen and unfrozen soil) and estimating the amount of liquid water in frozen ground. Further, GPR has the best potential resolving power of these geophysical techniques used to image shallow processes.

GPR has been effectively used for the characterization of a wide range of glacial and frozen environments (Woodward and Burk, 2007; Kneisel et al., 2008). Numerous studies have successfully used GPR to evaluate the spatial and temporal distribution of ground ice, depth to permafrost table and thickness of the active layer above the permafrost (e.g., Annan and Davis, 1978; Delaney et al., 1990; Arcone et al., 1998; Hinkel et al., 2001; Moorman et al., 2003; De Pascale et al. 2008). Recently, Kneisel et al. (2008) was able to image an upper and lower thermal interface delineating the lateral distribution of a seasonally unfrozen soil layer within a frozen soil environment of a water deltaic area. Wollschläeger et al. (2008) successfully applied multi-channel ground-penetrating radar to simultaneously map the depth to permafrost table and average moisture content in the active layer at a continuous permafrost site. These recent studies demonstrate the ability of GPR for distinguishing between frozen and unfrozen soil zones.

While there has been substantial work concerning the application of GPR for monitoring arctic and subarctic permafrost and seasonal frost environments, there has been very limited examination of the capacity of GPR to characterize very shallow (e.g., <1.0 m) mid-latitude freeze-thaw processes. Recently, Steelman and Endres (2009) demonstrated that the evolution of high-frequency GPR direct ground waves could be used to monitor the seasonal development of a very thin shallow frozen soil layer. In this paper, we present high-frequency GPR field data that monitors the seasonal (i.e., long-term) development and dissipation of a shallow soil frost zone overlying unfrozen wet substratum during a single winter season. Information about the state of frozen and unfrozen materials is derived from the use of common-midpoint (CMP) soundings while the imaging of spatial variations is achieved using fixed-offset reflection profiling. We also show that short duration mid-winter thawing events that commonly occur in mid-latitude conditions can be monitored using high-frequency GPR. These events result in the formation of

relatively thin thaw layers overlying frozen substrata, resulting in the occurrence of dispersive waveguides. Analysis of the observed dispersive wavefields in the GPR data yield information about these systems. These examples clearly demonstrate the suitability of high-frequency GPR for characterizing and monitoring the spatial and temporal development of very shallow freeze-thaw processes common to mid-latitude climates.

GPR BACKGROUND

GPR uses a transmitting antenna positioned along the surface (i.e., the air-ground interface) that radiates short pulses of electromagnetic (EM) waves commonly in the frequency band between 10 MHz and 1 GHz. These propagating EM waves respond to changes in material electrical properties and are recorded by a receiving antenna also located on the surface. GPR can be operated using bistatic antennas which allow the user to perform both fixed-offset reflection profiling and multi-offset CMP soundings. The conventional reflection profiling technique allows the user to collect a cross-sectional image of subsurface interfaces that delineate spatial changes in electrical properties. CMP surveys systematically separate a transmitting and receiving antenna about a central fixed point, which results in a separation of coherent events in the wavefield (e.g., direct air wave, direct ground wave and hyperbolic reflections). The direct ground wave propagates along the air-ground interface and is effectively sensitive to near-surface conditions (e.g., approximately one-half dominant wavelength in ground) while reflection events are affected by conditions along raypaths down to a given reflecting interface.

The propagation velocity (v) of EM waves within GPR bandwidth primarily depends on the relative dielectric permittivity (κ) of the material (i.e., the measured dielectric permittivity relative to the free space permittivity). This relationship is defined by the equation:

$$v = \frac{c}{\sqrt{\kappa}}, \tag{1}$$

where c is the electromagnetic velocity in free space (0.2998 m/ns). Many successful applications of GPR rely on the large electrical contrast between liquid water and the remaining subsurface components. Within the GPR bandwidth, the dielectric permittivity for most geophysical applications ranges between 1 (air) and 80 (liquid water). Table 1 provides a summary of dielectric permittivities and EM wave velocities for some typical materials. The large dielectric value of liquid water (80) relative to ice (3.2) provides a basis for monitoring freeze-thaw processes using EM wave velocity measurements. Further, an estimate of liquid water content can be obtained using an appropriate petrophysical relationship during these processes (e.g., Patterson and Smith, 1981; Stein and Kane, 1983; Nyberg et al., 2001).

Table 1. Typical values of relative dielectric permittivity and EM wave velocity for common geological material within GPR bandwidth. Source: [a] Reynolds (1997), [b] Moorman et al. (2003).

Material	Dielectric Permittivity κ	Typical Velocity (m/ns)
Air	1	0.2998
Ice[a]	3.2	0.167
Permafrost[a]	1-8	0.106 – 0.3
Dry Sand[a]	3-6	0.12 – 0.17
Wet Sand[a]	25-30	0.055 – 0.060
Frozen Sediment[b]	6	0.12
Unfrozen Sediment[b]	25	0.060
Water	80	0.033

The resolution of GPR techniques is determined by the wavelength of the emitted signal which is the product of the wave velocity and the dominant period of the electromagnetic pulse. Due to their short temporal period, higher frequency signals provide better resolution than lower frequency pulses. However, higher frequencies attenuate more rapidly and thus have a shallower depth of investigation. Hence, there is an inherent trade-off in the use of GPR between depth of investigation and signal resolution. Given the very shallow depth (<1.0 m) of the freeze-thaw processes being monitored and the relatively low attenuation in frozen soils, high-frequency GPR are an ideal method for high-resolution imaging of these phenomena.

Normal-moveout (NMO) velocity analyses applied to CMP soundings provide information about the subsurface EM wave velocity profile. The hyperbolic form of the offset distance-traveltime relationship for reflection events is the basis for methods used to determine the NMO velocity for a specific reflection event. Commonly used velocity analyses employ a semblance statistic which is a measure of signal coherency along the hyperbolic trajectory of a reflection event. The semblance statistic is expressed as the normalized output-to-input energy ratio on a velocity versus time plot, where semblance peaks correspond to NMO velocities and two-way zero-offset times for the reflection events (Yilmaz, 2001).

The NMO velocity for a given reflection is an average velocity value for the overlying material through which this event propagates. An interval velocity for the material located between two reflecting events can be obtained from the NMO velocity information using Dix (1955) equation:

$$v_{\text{int}} = \sqrt{\frac{v_L^2 t_L - v_U^2 t_U}{t_L - t_U}}, \tag{2}$$

where v_L and v_U are the NMO velocities of the lower and upper reflecting boundaries, while t_L and t_U are the corresponding two-way zero-offset traveltimes. Corresponding interval thickness between persistent reflection events (e.g., stratigraphic interfaces) or thermal interfaces is obtained from the measured traveltimes and interval velocity.

The amplitude of an EM wave will vary when it encounters an interface between materials with differing electrical properties. This change is due to the fact that when a wave impinges an interface some of the energy is reflected while the remaining energy is transmitted. The relative amplitude of a reflected wave is defined by the reflection coefficient (*R*) which primarily depends on the contrast in electrical properties. The reflection coefficient for a downward traveling normal incident signal is defined by:

$$R = \frac{\sqrt{\kappa_U} - \sqrt{\kappa_L}}{\sqrt{\kappa_U} + \sqrt{\kappa_L}}, \tag{3}$$

where κ_U is the dielectric permittivity of the upper (i.e., incident) layer while κ_L is the dielectric permittivity of the lower (i.e., refracting) layer. Reflection coefficients range between 1 and -1, where the negative sign convention denotes a reversal in the polarity of the reflected signal. The magnitude of *R* is directly related to the permittivity contrast at the interface; hence, large amplitude reflections indicate boundaries with a strong permittivity contrast.

SITE DESCRIPTION

The GPR field studies were conducted at two field sites located in southern Ontario, Canada (Figure 1). The Woodstock site (519845E, 4770361N) is characterized by silt loam soil (17% sand, 79% silt, 4% clay), while the Waterloo site (528878E, 4814702N) is characterized by sandy soil (97% sand, 3% silt). The mean annual air temperature and precipitation (1971–2000) in the region surrounding the Woodstock site is 7.5 ˚C and 954 mm; the atmospheric conditions over the same period for the region surrounding the Waterloo site is 6.7˚C and 908 mm, respectively (Environment Canada, 2008). In general, seasonal conditions in southern Ontario are

characterized by frozen soil conditions during the months of December–March and unfrozen conditions for the remainder of the year.

Figure 1. Study site locations in southern Ontario, Canada (revised from Natural Resources Canada, 2003).

The Woodstock site is situated in a localized valley portion of an active agricultural field characterized as a glacialfluvial outwash channel (Cowan, 1975). Core logs in the vicinity show that the monitoring location is characterized by approximately 0.5–0.7 m of silt loam grading downward into a silty gravel with sand. The water table is located 2–3 m below ground surface. The Waterloo site is situated on a relative topographic high within an active agricultural field located on top of the Waterloo moraine which is characterized as an irregular tract of gently rolling to hummocky terrain with some exposures of ice-contact stratified sand and gravel deposits (Bajc et al., 2004). The regional water table at the Waterloo site is located approximately 15–20 m below ground surface.

DATA COLLECTION

Continuous daily measurements of precipitation and atmospheric temperature for the Woodstock and Waterloo sites were collected at near-by weather stations during the 2007 and 2008 winter seasons, respectively. Conditions at the Woodstock site were monitored using an on-site meteorological station located approximately 0.5 km from the field site. Conditions at the Waterloo site were monitored from the University of Waterloo weather station located approximately 7 km east of the field site.

GPR data sets were collected at the Woodstock and Waterloo sites during the development of the seasonal soil frost zone and subsequent seasonal thaw (e.g., January–March). The relatively thin snow pack at each site (e.g., <0.3 m) was removed prior to conducting the GPR surveys. CMP soundings and reflection profiling were concurrently conducted along a fixed survey line using a Sensors and Software PulseEKKO™ 1000 GPR system (Sensors and Software Inc., Mississauga, ON, Canada) equipped with 900 MHz bistatic antennas. The GPR data was collected using a time window of 100 ns, sampling interval of 0.1 ns and 64 stacks per trace.

CMP soundings and reflection profiling at the Woodstock site were conducted on eight different dates between 13 January 2007 and 13 April 2007. CMP data was acquired over the range of antenna offsets from 0.2 m to 2.0 m using a 0.02 m step interval; corresponding reflection profiles were collected along a 2.0 m line using a spatial step size of 0.02 m. CMP soundings and

reflection profiling at the Waterloo site were conducted between 11 November 2007 and 26 April 2008; however, the GPR data pertaining to this study are focused on a single mid-winter thawing event occurring between 24 January and 8 February 2008). For this site, CMP data were acquired over the range of antenna offsets from 0.2 m to 4.0 m using a 0.02 m step interval; corresponding reflection profiles were collected along an 8.0 m line using a spatial step size of 0.02 m. For both data sets, the midpoint location of the CMP surveys coincides with the center of the corresponding reflection profile.

The following processing sequence was applied to the GPR data sets: 1) Dewow filter to remove low-frequency signal saturation, 2) time zero correction, 3) bandpass temporal filtering with 100, 200, 1100, 1400 MHz (i.e., low cut frequency, lower plateau, upper plateau and high cut frequency), 4) spreading and exponential compensation (SEC) gains to compensate for geometrical spreading and attenuation losses and 5) time-to-depth conversion for reflection profiles. It should be noted that identical gains were applied to a sequence of GPR measurements collected at particular location (e.g., the same gain function was applied to the CMP soundings collected at the Woodstock site), thereby permitting a comparison of relative reflection amplitudes.

FIELD OBSERVATIONS

High-frequency GPR data acquired during this study clearly demonstrates the ability of this non-invasive technique to monitor and characterize differing aspects of the freeze-thaw process. Conditions during the 2007 winter seasonal period at the Woodstock site are well described in terms of a single, long-term freeze and thaw cycle; daily average temperatures were persistently sub-zero between 9 January 2007 and 21 March 2007. Temporal GPR data collected at the Woodstock site during this period show the development of a relatively thick, seasonal frost layer and the occurrence of the subsequent infiltration event during the seasonal thaw.

In contrast, a number of short-term (i.e., 1–5 day) mid-season thawing events occurred during the 2008 winter seasonal period at the Waterloo site. The formation of a relatively thin, thawed layer (e.g., near or less than the dominant wavelength of GPR) over a frozen substratum gave rise to a unique wave propagation phenomenon called a dispersive waveguide. Analysis of these dispersive waveguides yield estimates of the properties of the unfrozen and frozen layers.

Seasonal Velocity Variations

CMP data collected at the Woodstock site during the 2007 winter seasonal period are shown in Figure 2. The CMP soundings (upper series of panels) were analyzed using the semblance statistic (middle series of panels) which was then used to construct a velocity-depth profile (lower series of panels) for each of the soundings. These vertical velocity profiles were derived from three coherent reflection events; the NMO velocity picks corresponding to these reflection events are shown on the semblance plots.

The initial CMP sounding (Figure 2a) was conducted on 13 January 2007 during unfrozen wet soil conditions. Daily average atmospheric temperatures were consistently below zero after 9 January 2007; however, the seasonal snowpack was not yet developed at this time. The GPR data displays a strong, well-developed low velocity direct ground wave (DGW) with an increasing velocity with depth. During this period, the upper soil interval was characterized by a relative low velocity of 0.062 m/ns.

The CMP sounding collected on 22 January 2007 (Figure 2b) was conducted after the formation of a relatively thin (e.g., <0.05 m) snowpack. The occurrence of an attenuated DGW is indicative of the formation of a thin frozen soil layer (i.e., thin relative to dominant GPR wavelength) over an unfrozen substratum (Steelman and Endres, 2009). This inference is supported by a velocity increase to 0.079 m/ns in the uppermost soil interval which is consistent with the presence of high velocity frozen soil within this layer.

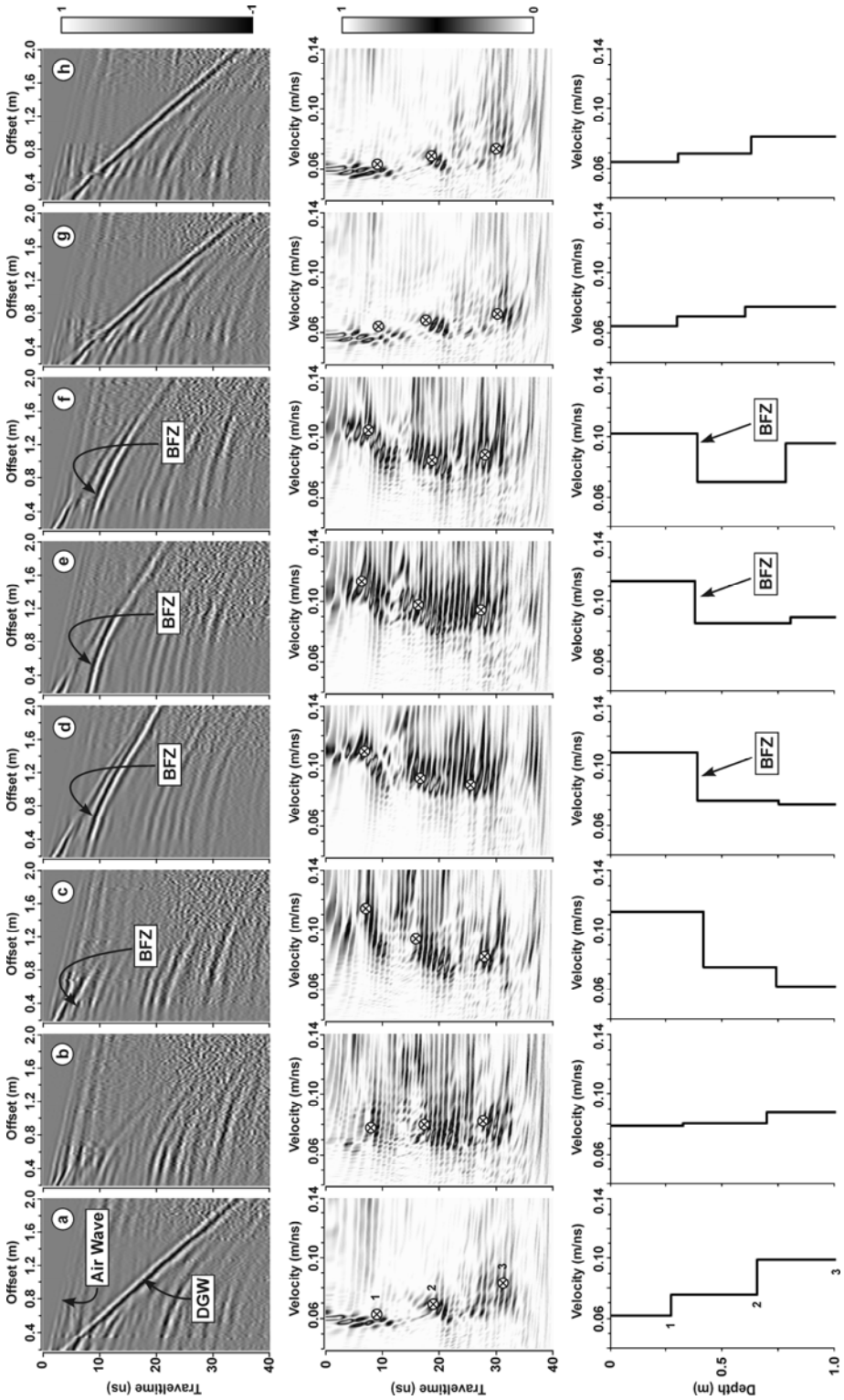

Figure 2. CMP soundings (upper panels), semblance plots (middle panels) and interval velocity models (lower panels) obtained at the Woodstock study site during the development of a surficial frozen soil layer and subsequent seasonal thaw. The three NMO velocity picks identified on the semblance plots were used to calculate the interval velocity models. Surveys were conducted on (a) 13 January 2007, (b) 22 January 2007, (c) 31 January 2007, (d) 20 February 2007, (e) 5 March 2007, (f) 21 March 2007, (g) 28 March 2007 and (h) 13 April 2007.

The CMP sounding acquired on 31 January 2007 (Figure 2c) shows the effects of the continued freezing process with the emergence of a pronounced high velocity DGW and a further velocity increase in the upper soil interval to 0.11 m/ns. This CMP sounding also contains a strong reflection event at approximately 4 ns (an approximate depth of 0.22 m); its polarity is consistent with a velocity decrease with depth (e.g., a high velocity frozen layer over a lower velocity unfrozen substratum). Given its polarity and the associated high velocity in the near-surface, this event is interpreted to be the base of the soil frost zone (BFZ).

The following CMP soundings collected on 20 February 2007 (Figure 2d) and 5 March 2007 (Figure 2e) both continue to show well-developed high velocity DGW and high velocity conditions in the upper soil interval (e.g., 0.11 m/ns). The strong BFZ reflection event in the CMP sounding data has shifted to a later traveltime (~7 ns), indicating a downward migration of the BFZ to a depth of 0.40–0.43 m. It should also be noted that the snowpack was at its maximum height (e.g., 0.3–0.5 m) during this period.

The CMP sounding done on 21 March 2007 (Figure 2f) was conducted at the end of the seasonally sub-zero period. The snowpack was completely melted as a result of sufficiently high daily temperatures prior to this survey date. In addition, an intense short-term overland flow event that covered our site with about 0.5 m of meltwater was observed on 13 March 2007. The velocity analysis found only a slight decrease in velocity for the upper soil intervals (to 0.10 m/ns), and the BFZ event was readily observed at a depth of 0.42 m. These results show the continued presence of the frozen soil layer after the major snowpack melt. The final two CMP soundings collected on 28 March 2007 (Figure 2g) and 13 April 2007 (Figure 2h) show a return to low velocity conditions across the entire depth interval (e.g., 0.064–0.082 m/ns) indicative of wet unfrozen soil conditions (e.g., increasing velocity with depth).

Spatial Imaging of Freeze-Thaw Process

While CMP soundings can be used to obtain substratum physical properties, they do not provide information about the spatial development of freeze-thaw interfaces. The GPR reflection profiles corresponding to the CMP soundings discussed above are presented in Figure 3. It should be noted that the vertical axis for these profiles has been converted into a depth estimate for the reflecting boundaries using the corresponding interval velocity information provided in Figure 2.

Figure 3a shows the reflection profile obtained during the unfrozen soil conditions on 13 January 2007. Its notable feature is the strong first arrivals which are a composite event consisting of the direct air and DGW. By the time of the profiling on 22 January 2007 (Figure 3b), the freezing process has commenced; however, it appears that the soil frost front is too shallow to generate a reflection event that has sufficient two-way traveltime to appear as a distinct event below the composite first arrival event. In this case, the interference between these overlapping events obscures the frost front reflection.

Profiling on 31 January 2007 (Figure 3c) starts to image a distinct frost line reflection across the survey line at a depth of approximately 0.20 m. This event correlates with the BFZ reflection noted at 4 ns on the corresponding CMP data (Figure 2c). After a substantial period of freezing conditions, the reflection profiling on 20 February 2007 (Figure 3d) shows that the BFZ event has descended to depths varying between 0.28–0.40 m across the profile line. By 5 March 2007 (Figure 3e), the BFZ event continued downward to 0.38–0.43 m depth across the profile line. During this later period, the profile also displays a significant increase in the reflection amplitude of the BFZ event.

Profiling done on 21 March 2007 (Figure 3f) continued to image the BFZ event at depths between 0.28–0.42 m, supporting the CMP sounding results that indicated the continued presence of a frozen surface layer. However, the relative amplitude of the reflection event appears to be slightly diminished compared to the previous measurement period.

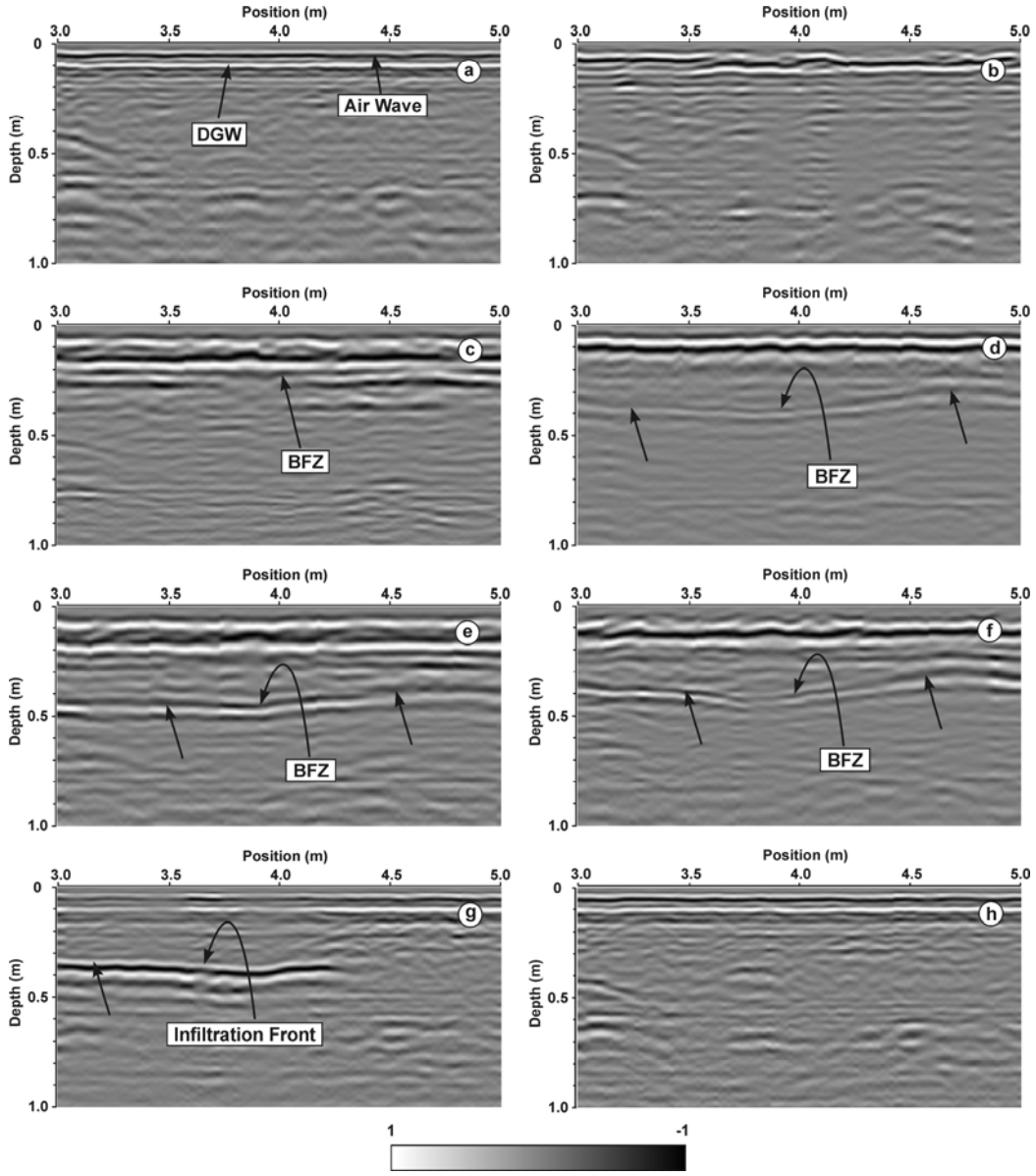

Figure 3. Reflection profiles collected at the Woodstock site. Profiles were concurrently collected with the CMP soundings on (a) 13 January 2007, (b) 22 January 2007, (c) 31 January 2007, (d) 20 February 2007, (e) 5 March 2007, (f) 21 March 2007, (g) 28 March 2007 and (h) 13 April 2007. Vertical time axis was transformed to depth using the velocity information obtained from CMP velocity analysis.

The reflection profile acquired one week later on 28 March 2007 (Figure 3g) shows drastic changes in reflection character. In particular, the strong reflection that is present has an opposite polarity compared to the reflection from the BFZ. This polarity change indicates a reversal in the sense of the electrical properties contrast for this reflection event. The character of this reflecting interface suggests that it represents an infiltration front associated with release of liquid water due to the thawing of the near-surface frozen zone. The final reflection profile conducted on 13 April 2007 (Figure 3h) shows a return to thawed conditions similar to those encountered at the start of this sequence on 13 January 2007 (i.e., Figure 3a).

Near-Surface Waveguide

GPR field investigations at the Waterloo site during the 2008 winter seasonal period was characterized by multiple mid-season freeze-thaw cycles, which resulted in the formation of transient thin surface thaw zones underlain by frozen and/or partially frozen sediment. During these periods, wave dispersion was readily observed in the GPR data. Wave dispersion will occur when wave energy is repeatedly reflected within a waveguide, which results in a series of multiples that manifest into a package of dispersed waves (van der Kruk et al., 2006). Arcone (1984) showed that GPR wave dispersion could develop for a thin layer bounded by two confining layers with contrasting dielectric permittivities (e.g., ice bounded by air and water), and would essentially propagate as lossless dispersive waves for layer thickness near or less than the in-situ wavelength at velocities that may not correspond to the layer's dielectric properties (Arcone et al., 2003).

The thickness of the thin thawed layers is below the resolving power of the conventional reflection profiling and CMP velocity analyses discussed above. However, the effects of these dispersive shallow waveguides can be observed in both profiling and CMP data. Further, analysis of these dispersed modes can yield layer thickness and layer dielectric properties (e.g., van der Kruk et al., 2007). Results of van der Kruk et al. (2009) readily demonstrate the dispersion inversion technique for estimating thin frozen and thawed soil properties using high-frequency 900 MHz CMP data sets.

Figure 4a shows a CMP sounding collected on 24 January 2008 at the Waterloo site after a period of prolonged freezing conditions. The sounding is characterized by a well-developed DGW across the entire range of offsets as well as a high amplitude hyperbolic reflection event at approximately 7 ns. This reflection event is interpreted to represent the BFZ, which yielded a NMO velocity and depth to interface of 0.15 m/ns and 0.72 m, respectively. Relatively persistent sub-zero atmospheric conditions were observed until 5 February 2008, at which time temperatures increased causing a short-duration thawing period. These conditions were subsequently followed by a return to sub-zero atmospheric conditions and further snowfall accumulation on 6 and 7 February 2008. The CMP sounding collected on 8 February 2008 (Figure 4b) was completely different than the sounding collected on 24 January 2008, and was characterized by highly dispersive wave propagation across the entire offset range; this type of wave phenomenon was commonly observed for periods of 1–5 days following the initiation of surface thawing conditions during the course of the 2008 winter season.

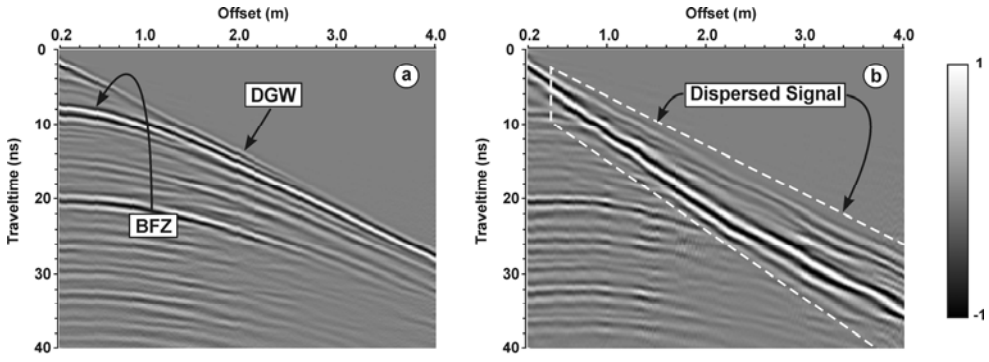

Figure 4. CMP soundings collected at the Waterloo site on (a) 24 January 2008 during frozen soil conditions and on (b) 8 February 2008 following a mid-seasonal thawing event.

Here, we employ the inversion procedure introduced by van der Kruk et al. (2009) for thin thaw layers overlying frozen substratum; details of this procedure are thoroughly discussed in van der Kruk et al. (2006). The inversion analysis applied to the CMP data collected on 8 February 2008 involved calculating the phase-velocity spectra, followed by the determination of the dispersion curve corresponding to the fundamental dispersion mode. This dispersion curve was then inverted for a single layer model to obtain the EM wave velocity of the thawed layer waveguide, the

thickness of the thaw layer and the EM wave velocity of the underlying frozen substratum. The inversion results shown in Figure 5 yielded a thawed layer dielectric permittivity and thickness of 10.3 (i.e., v = 0.09 m/ns) and 0.06 m, respectively, and a frozen layer dielectric permittivity of 4.3 (i.e., v = 0.14 m/ns).

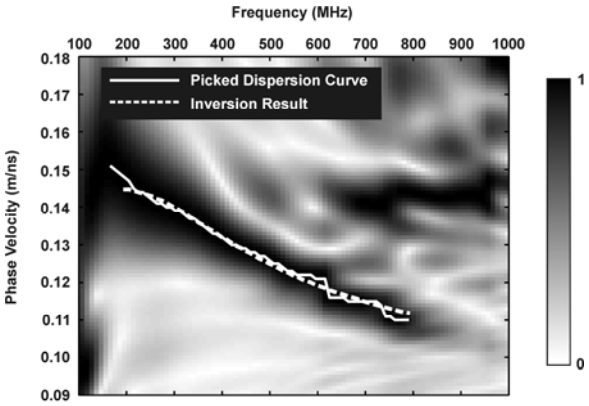

Figure 5. Phase velocity spectra of the CMP data collected on 8 February 2008 at the Waterloo site (Figure 4b). The solid line represents the picked dispersion curve while the dotted line is the dispersion curve calculated for the model parameters obtained from the inversion.

The thawing process also produced small-scale heterogeneities that resulted in near-surface scattering which were observed on the reflection profiles in the form of steeply inclined diffractions. Because these scattered waves travel in the shallow thawed waveguide, they also exhibit a dispersive character. Previous field studies by Moorman et al. (2003) noted similar steeply dipping diffraction events on GPR profiles collected across relatively thin shallow thaw zones (e.g., less than the resolving capability of the GPR) overlying frozen sediment. Moorman et al. attributed these near-surface diffractions to shallow point source reflectors which they used to delineate small ice lenses; however, they did not note that these events were dispersive in character.

Figure 6 shows the two reflection profiles corresponding to the CMP surveys collected at the Waterloo site. The profile collected on 24 January 2008 (Figure 6a) represents a typical image acquired when a well-developed frozen surface is present. The laterally continuous, high amplitude reflection from the BFZ is located at approximately 6–8 ns on the traveltime profile. This event correlates with the reflection identified in Figure 4a. At this time, no near-surface scattering is present on the profile. However, the profile collected on 8 February 2008 (Figure 6b) is characterized by numerous near-surface diffractions which are dispersive in character. The presence of these dispersive diffractions is consistent with those observed in the corresponding CMP data (Figure 4b). While the BFZ event appears to be laterally continuous, the reflector is less pronounced and occurs at a slightly later traveltime (e.g., 9–10 ns) that is consistent with the presence of overlying lower velocity thawed material. Analysis of these diffraction events may yield valuable information of near-surface physical properties analogous to that obtained from the CMP soundings. However, the inversion of dispersive waveguide events obtained from reflection profiling is a topic of future research.

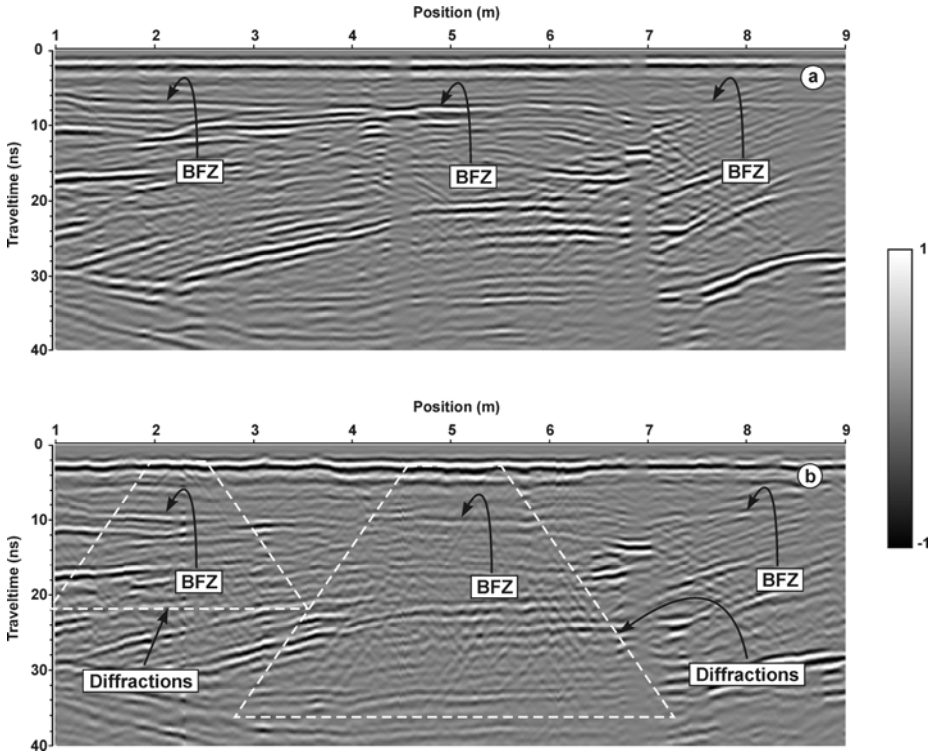

Figure 6. Reflection profiles collected at the Waterloo site on (a) 24 January 2008 during surficially frozen soil conditions and on (b) 8 February 2008 following a mid-seasonal thawing period.

SUMMARY

While numerous studies have shown GPR to be an effective tool for the characterization of a wide range of glacial and permafrost environments, there have been very limited studies in highly variable mid-latitude environments characterized by very shallow freeze-thaw processes. To demonstrate the capability of GPR for monitoring and characterizing freeze-thaw processes, field data is presented for a single long-term (e.g., 3 month) seasonal freeze and thaw cycle in 2007 and a short-term (e.g., 1–5 day) mid-season thawing event in 2008.

Time-lapse GPR surveys collected at the Woodstock site successfully characterized seasonal variations due to shallow freeze and thaw processes. For example, CMP soundings were used to characterize the temporal development of the seasonal frost zone in the upper 0.5 m of soil, where both the frozen layer properties and depth to frost base were characterized. The corresponding reflection profiles successfully imaged the spatial position of the base of the frost zone, as well as the base of the subsequent seasonal infiltration front at the end of the winter season.

The GPR surveys at the Waterloo site were used to characterize freeze and thaw processes in the very shallow soil surface (e.g., less than the dominant wavelength of GPR). During a short-duration thawing event, highly dispersive wave propagation was observed in both the CMP and reflection profile data. An inversion procedure was used to obtain the physical properties of the unfrozen waveguide layer and underlying frozen substratum. While the inversion procedure was successfully demonstrated for the CMP data set, the application of this inversion procedure for dispersive events observed in reflection profiles will be the topic of future work.

In this paper, we have clearly shown the potential capabilities of high-frequency GPR for the temporal and spatial characterization of very shallow freeze and thaw processes. It can be seen that these field techniques can supply valuable information that would improve our understanding of their impact on hydrological processes.

ACKNOWLEDGEMENTS

This work was supported by a Post Graduate Scholarship (PGS-M and PGS-D) to Mr. Colby Steelman and an Individual Discovery Grant to Dr. Anthony Endres from the Natural Sciences and Engineering Research Council of Canada (NSERC), and by a grant from ETH Zurich. We would also like to thank Alicia and Murray Smith for permission to use the Waterloo site for this study.

REFERENCES

Annan AP. Davis JL. 1978. High frequency electrical methods for the detection of freeze-thaw interfaces. In *Proceedings of the Third International Conference on Permafrost* **1**: 495 – 500.

Arcone SA. 1984. Field observations of electromagnetic pulse propagation in dielectric slabs. *Geophysics* **49**: 1763 – 1773.

Arcone SA. Lawson DE. Delaney AJ. Strasser JC. Strasser JD. 1998. Ground-penetrating radar reflection profiling of groundwater and bedrock in an area of discontinuous permafrost. *Geophysics* **63**: 1573 – 1584.

Arcone SA. Peapples PR. Liu L. 2003. Propagation of a ground-penetrating radar (GPR) pulse in a thin-surface waveguide. *Geophysics* **68**: 1922 – 1933. DOI: 10.1190/1.1635046.

Bajc AF. Endres AL. Hunter JA. Pullan SE. Shirota J. 2004. Three-dimensional mapping of quaternary deposits in the Waterloo Region, southwestern Ontario. In: Berg RC. Russell HAJ. Thorleifson LH: (Editors). Three-Dimensional Mapping for Geological Applications Workshops, Illinois State Geological Survey, Open File Series 2004-8, St. Catharines, Ontario, Canada, Associated with the 2004 Geological Association of Canada Meeting, pp. 12-15.

Bayard D. Stähli M. Parriaux A. Flühler H. 2005. The influence of seasonally frozen soil on the snowmelt runoff at two Alpine sited in southern Switzerland. *Journal of Hydrology* **309**: 66 – 84. DOI: 10.1016/j.jhydrol.2004.11.012.

Cowan WR. 1975. Quaternary geology of the Woodstock area. Southern Ontario. Ontario. Ministry of Natural Resources, Division of Mines. vii, 91p.

Delaney AJ. Arcone SA. Chacho Jr EF. 1990. Winter short-pulse studies on the Tanana River, Alaska. *Arctic* **43**: 244 – 250.

De Pascale GP. Pollard WH. Williams KK. 2008. Geophysical mapping of ground ice using a combination of capacitive coupled resistivity and ground-penetrating radar, Northwest Territories, Canada. *Journal of Geophysical Research* **113**: F02S90. DOI: 10.1029/2006JF000585.

Dix CH. 1955. Seismic velocities from surface measurements. *Geophysics* **20**: 68 – 86.

Environment Canada. "National Climate Data and Information Archive – Canadian Climate Normals, 1971 – 2000". 2008-11-01. 2009-04-27 <http://www.climate.weatheroffice.ec.gc.ca/climate_normals/index_e.html>

Hayhoe HN. Bailey WG. 1985. Monitoring changes in total and unfrozen water content in seasonally frozen soil using time domain reflectometry and neutron moderation techniques. *Water Resources Research* **21**: 1077 – 1084.

Hinkel KM, Doolittle JA. Bockheim JG. Nelson FE. Paetzold R. Kimble JM. Travis R. 2001. Detection of subsurface permafrost features with ground-penetrating radar, Barrow, Alaska. *Permafrost and Periglacial Processes* **12**: 179 – 190. DOI: 10.1002/ppp.369.

Johnsson H. Lundin LC. 1991. Surface runoff and soil water percolation as affected by snow and soil frost. *Journal of Hydrology* **122**: 141 – 159.

Kneisel C. Hauck C. Fortier R. Moorman B. 2008. Advances in geophysical methods for permafrost investigations. *Permafrost and Periglacial Processes* **19**: 157 – 178. DOI: 10.1002/ppp.616.

Moorman BJ. Robinson SD. Burgess MM. 2003. Imaging periglacial conditions with ground-penetrating radar. *Permafrost and Periglacial Processes* **14**: 319 – 329. DOI: 10.1002/ppp.463.

Natural Resources Canada. "The Atlas of Canada – Ontario". 2003-03-14. 2009-05-01 <http://atlas.nrcan.gc.ca/site/english/maps/reference/outlineprov_terr/ont_outline>

Nyberg L. Stähli M. Mellander PE. Bishop KH. 2001. Soil frost effects on soil water and runoff dynamics along a boreal forest transect: 1. field investigations. *Hydrological Processes* **15**: 909 – 926. DOI: 10.1002/hyp.256.

Patterson DE. Smith MW. 1981. The measurement of unfrozen water content by time domain reflectometry: results from laboratory tests. *Canadian Geotechnical Journal* **18**: 131 – 144.

Reynolds JM. 1997. *An Introduction to Applied and Environmental Geophysics.* John Wiley & Sons: West Sussex, England; 796.

Steelman CM. Endres AL. 2009. Evolution of high-frequency ground-penetrating radar direct ground wave propagation during thin frozen soil layer development. *Cold Regions Science and Technology* **57**: 116 – 122. DOI: 10.1016/j.coldregions.2009.01.007.

Stein J. Kane DL. 1983. Monitoring the unfrozen water content of soil and snow using time domain reflectometry. *Water Resources Research* **19**: 1573 – 1584.

van der Kruk J. Steelman CM. Endres AL. Vereecken H. 2009. Dispersion inversion of electromagnetic pulse propagation within freezing and thawing soil waveguides. *Geophysical Research Letters*, DOI: 10.1029/2009GL039581, in press.

van der Kruk J. Streich R. Green AG. 2006. Joint dispersion inversion of broadside and endfire CMP georadar data for properties of a thin-surface waveguide. *Geophysics* **71**: K19 – K29. DOI: 10.1190/1.2168011.

van der Kruk J. Arcone SA. Liu L. 2007. Fundamental and higher mode inversion of dispersed GPR waves propagating in ice layer. *IEEE Transactions on Geoscience and Remote Sensing* **45(8):** 2483 – 2491. DOI: 10.1109/TGRS.2007.900685.

Wollschläeger U. Gerhards H. Yu Q. Roth K. 2008. Application of multi-channel ground-penetrating radar to determine thaw depth and moisture content of the active layer. *Eos Trans. AGU* **89(53):** Fall Meet. Suppl. Abstract C31E-0545.

Woodward J. Burke MJ. 2007. Applications of ground-penetrating radar to glacial and frozen materials. *Journal of Environmental Engineering Geophysics* **12**: 69 – 85.

Yilmaz O. 2001. Seismic Data Analysis: Processing, Inversion, and Interpretation of Seismic Data (Volume 1). Society of Exploration Geophysicists: Tulsa Oklahoma; 1000.